Phase diagram of the five-vertex model

Miklós Gulácsi
*Scuola Internazionale Superiore di Studi Avanzati, Strada Costiera 11, Miramare, 34014 Trieste, Italy and Theoretical Division, Los Alamos National Laboratory, Los Alamos, New Mexico 87545**

Henk Van Beijeren
Institute for Theoretical Physics, University of Utrecht, The Netherlands

Andrea C. Levi
*Scuola Internazionale Superiore di Studi Avanzati, Strada Costiera 11, Miramare, 34014 Trieste, Italy and Universitá di Genova, Dipartimento di Fisica, 16146 Genova, Italy**

(Received 13 October 1992)

Within the ice-type models, the solution of the five-vertex model is obtained with the use of the Bethe ansatz. Since the allowed number of vertex types is odd, the arrow-reversal symmetry of the system is broken by construction. Due to this, the exact solution obtained and the phase diagram are very different from those of the symmetric six-vertex model. A connection to the asymmetric six-vertex model (of which the five-vertex model is an extreme case) is made. The different regions of the phase diagram are described and the transitions between them are analyzed. Several aspects of the phase diagram are unusual, i.e., the ordered phases (both ferroelectric and antiferroelectric) are frozen-in phases and the disordered phase is replaced by a ferrielectric phase. In the free-fermion case, the known results of the modified potassium dihydrogen phosphate model are recovered.

PACS number(s): 05.50.+q, 64.60.Cn, 64.60.Fr, 68.35.Rh

I. INTRODUCTION

The two-dimensional lattice models of interacting systems which were exactly solved can be regarded as special cases of a more general (and in general unsolved) "interaction-around-a-face" model. From another point of view, they can be regarded as extensions of the Ising model. Thus all of them can be solved also by the transfer-matrix method (for the Ising [1] and dimer [2, 3] models the transfer matrix reduces to Pfaffian equations) [4]. Subsequently it was realized [5, 6] that the triangular three-spin [7] and hard-hexagon models [8] are special cases of the eight-vertex model [9] and the self-dual Potts model [10] is equivalent [11] to the six-vertex model [12]. (Note that the six-vertex model without an external electric field can be related to a critical limit of the eight-vertex model [13, 14].) Consequently, we are then left [15] with two distinct exactly solvable vertex models in two dimensions [16, 17], that is, the six- and the eight-vertex model. Here we will be mainly interested in the six-vertex model.

The vertex models define a statistical mechanics on a lattice (for simplicity, a square lattice) as follows. On each link there is a variable taking two values that is represented (in the conventional representation) by an arrow, i.e. $\rightarrow$ or $\leftarrow$, or equivalently (in the so-called *line representation*) by an *empty* or *full* line, respectively. To each vector therefore there correspond $2^4 = 16$ possible configurations. To each of these we associate a Boltzmann weight $\omega_i = \exp(-\beta\varepsilon_i)$. This general model is referred to as the sixteen-vertex model. It is equivalent to an Ising model with two-, three- and four-body interactions and with an external magnetic field [18]. The exact solution of this general ferroelectric model is not known. Only in two cases we know of, the system will exhibit an Ising-like transition. These two cases are obtained [19] by a specific choice of the Boltzmann weights which leads inevitably to an Ising model with only two-body interactions.

If we choose the Boltzmann weights so that six vertices with two entering and two exiting arrows have finite weight, then we define the six-vertex model, historically known as an *ice-type* model [20]. In the following, we will adopt the traditional [21, 22] ordering of the vertices [23]. After its exact solution was known [12, 21, 22], the six-vertex model had been extensively used in numerous statistical-mechanical problems. One of the most useful is surface modeling [24], i.e., the description of the equilibrium shape of a crystal and of surface growth.

An important class of models, frequently used for a crystal-vapor interface, obeys the solid-on-solid (SOS) condition [25]. The atoms are assumed to be densely packed in a lattice; at the interface the condition stipulates that every atom must sit on top of another, so that *overhangs* and vacancies are excluded. Since neither the bulk of the crystal so defined nor the vapor contribute any degrees of freedom to the system, the model merely describes the crystal-gas interface in a simplified form. It turns out that some versions of the SOS model, which correspond to certain surfaces (faces) of well-defined crystals, are isomorphic to the six-vertex model. For example the body-centered solid-on-solid (BCSOS) model [24, 26] is suitable for the description of the (001) face of a bcc crystal. The model can be also extended to model the

(001) face or the (011) face [27, 28] of a fcc crystal.

A new method, which differs from the previous mapping scheme, was introduced recently [29] to describe the surfaces of crystals with rectangular (in particular, cubic) symmetry. The only allowed perturbations of a perfectly flat surface are noncrossing steps. Let us consider the line representation [21, 22] of the allowed arrow configurations of the six-vertex model. Performing the mapping procedure of Ref. [29], the step lines on the crystal surface can be identified with the *fermion* lines occurring in the six-vertex model. If multiple steps emerge, a sliding procedure can be applied [29] to guarantee the presence of only single steps on the crystal surface. However, after application of the sliding procedure no touching of lines will occur. This is an important observation since, as a consequence, vertex two is actually absent from the six-vertex representation of the surface model.

A *five-vertex* model emerges in the representation of crystal-growth models. As just noted, some variants of the terrace-ledge-kink [30] model are isomorphic [29] to a five-vertex model. This becomes evident if we keep in mind that inclusion of vertex two would allow multiple steps to develop and cavities to appear which are not allowed in the terrace-ledge-kink growth model. In a different model of crystal growth [31], the five-vertex model can be viewed as a probabilistic cellular automaton. Physically it describes the surface slope of a crystal growing through deposition [31]

Based on these physical motivations we were led to look for an exact solution of a five-vertex model. This is the motivation of the present paper, which is organized as follows. In Sec. II we briefly present the Bethe-ansatz exact solution of the five-vertex model. The analytic properties of the solution and its connection to the asymmetric six-vertex model are also discussed. In Sec. III the free-fermion solution is revisited. Section IV is entirely devoted to the study of the phase diagram. The effect of an external field, the study of the correlations, and the connection of the model to SOS surfaces will be presented in a future publication.

II. BETHE-ANSATZ SOLUTION

In the general six-vertex model, all the six local arrangements will have distinct energies: $\varepsilon_1,\ldots,\varepsilon_6$, keeping the traditional ordering of the six vertices [21, 22]. The technique to obtain an exact solution with the coordinate Bethe ansatz is well known [21, 15, 32]; we will just briefly present the results. Let each row in the $N \times N$ square lattice consist of $N-n$ up arrows and n down arrows. The eigenvalue [33] of the general six-vertex model in terms of fugacities ($z_j = \exp ik_j$) is

$$\Lambda = \omega_1^N \prod_{i=1}^{n}\left[\omega_3 + \frac{\omega_5\omega_6 z_i}{\omega_1 - \omega_4 z_i}\right] + \omega_4^N \prod_{i=1}^{n}\left[\omega_2 - \frac{\omega_5\omega_6}{\omega_1 - \omega_4 z_i}\right] . \quad (1)$$

The sets $\{k_1, k_2, \ldots, k_n\}$ of n wave numbers k_j, obey the equation

$$z_i^N = (-1)^{n-1} \prod_{j=1}^{n} \frac{\omega_1\omega_3 + \omega_2\omega_4 z_i z_j - (\omega_1\omega_2 + \omega_3\omega_4 - \omega_5\omega_6) z_i}{\omega_1\omega_3 + \omega_2\omega_4 z_i z_j - (\omega_1\omega_2 + \omega_3\omega_4 - \omega_5\omega_6) z_j} . \quad (2)$$

There are only four independent energies to consider: this is because the zero of energy can be chosen arbitrarily, and the ice rule implies that $\varepsilon_5 = \varepsilon_6$ is no restriction [34].

For the five-vertex case it is actually enough to consider three independent Boltzmann weights, i.e., letting $\omega_2 = 0$, there exist three independent ratios among ω_1, ω_3, ω_4, and ω_5. In these conditions we will solve the general five-vertex model [35]. Our solution will be more general than the one derived previously by Wu [36], i.e., not limited to the free-fermion case $\omega_3\omega_4 = \omega_5\omega_6$. In the present (field-free) case, however, we still keep $\varepsilon_4 = \varepsilon_3$. Hence the independent parameters reduce to two: $x = \omega_1/\omega_5$ and $y = \omega_3/\omega_5$.

The noninteracting case had been solved [36] by a completely different technique, i.e., the Pfaffian method, using the equivalence of the present problem to that of close-packed dimers on a hexagonal lattice (it was known already from Kasteleyn's work on dimer statistics [2] that a phase transition exists). For this case Garrod also computed the correlations between arrows [29].

In the *symmetric* six-vertex model [12, 21, 22], the further conditions $\varepsilon_1 = \varepsilon_2$ and $\varepsilon_3 = \varepsilon_4$ are imposed. In this way the model is unchanged by reversing all dipole arrows, which one would expect to be the situation for a model in zero external field. To get insight in the five-vertex case from the six-vertex model one has to consider the latter in a direct field [37] (i.e., the so-called asymmetric six-vertex model) and to perform certain limits, where the field and the vertex energies have to approach infinity simultaneously (see Appendix A). The textbook solution [37] of the asymmetric six-vertex model uses [32, 37] several changes of variables, which are such as to ensure that the model will be symmetric with respect to reversing all arrows and the external field. This makes the five-vertex limit (see Appendix A) difficult to handle; in addition those changes of variables are not the most practical ones for handling the five-vertex limit. Therefore, hereafter, we resort to a direct solution of the five-vertex model by applying the Bethe ansatz afresh.

If $\omega_2 = 0$ the consistency equation [Eq. (1)] becomes

$$z_i^N = (-1)^{n-1} \prod_{j=1}^{n} \frac{1 - \Delta_5 z_i}{1 - \Delta_5 z_j} . \quad (3)$$

The interaction constant of the five-vertex model Δ_5 is defined as

$$\Delta_5 = \frac{\omega_3^2 - \omega_5^2}{\omega_1\omega_3} . \quad (4)$$

Let us first analyze Eq. (3), which can be written in the form

$$\frac{(1-\Delta_5 z_i)^n}{z_i^N} = (-1)^{n-1}\prod_{j=1}^{n}(1-\Delta_5 z_j)\ . \qquad (5)$$

Writing Eq. (5) for all $z_1, \ldots, z_n$ and multiplying the left-hand sides and the right-hand sides of the n equations thus obtained we get

$$z_1 z_2 \cdots z_{n-1} z_n = \tau\ , \qquad (6)$$

with τ being a Nth root of unity. Using

$$z_j = e^{ip_j} = e^{r_j} e^{i\,k_j}\ , \qquad (7)$$

that is, $p_j = k_j - ir_j$, for any N and n the r_j's and the k_j's satisfy

$$\sum_{j=1}^{n} r_j = 0\ ,$$
$$N\sum_{j=1}^{n} k_j = 2\pi m,\quad m = 0, 1, \ldots, N-1\ . \qquad (8)$$

The property stipulated by Eq. (8) was expected to hold, as it holds in any integrable model [38]. The points described by the function $1-\Delta_5 z_j$ [see Eq. (3)] lie on a circle of radius $\Delta_5 e^{r_j}$ with the center at the point $\mathrm{Im}z = 0$, $\mathrm{Re}z = 1$. Thus the following transformation [38] can be performed

$$e^{i\Theta(p,q)} = \frac{1-\Delta_5 e^{ip}}{1-\Delta_5 e^{iq}}\ . \qquad (9)$$

The analytic properties of $\Theta(p,q)$ are analyzed in Appendix B. As it can be seen the kernel is degenerate. Thus, on one hand, we have a simpler case than that of the symmetric six-vertex model, due to the degenerate kernel. But, on the other hand, the evaluation of the free energy will be more envolved than its symmetric six-vertex counterpart, due to the fact that the kernel is not unimodular.

It is very instructive to consider the case $n = 2$. From Eq. (3) we obtain

$$\Delta_5(z^{N-1} + z_1) = z_1^N + 1\ . \qquad (10)$$

The above equation is identical to that of the symmetric six-vertex case [22], with the obvious replacement of Δ_6 with Δ_5. The solution of Eq. (10) is well established [22]: if $\Delta_5 < 1$, Eq. (10) has one real solution and no pure imaginary solution; if $\Delta_5 > 1$, Eq. (14) has no real solution, but has a single positive imaginary solution.

Using Eq. (9), from Eq. (3) we obtain

$$\exp(iNp_l) = (-1)^{n-1}\prod_{j=1}^{n}\exp[i\Theta(p_l, p_j)]\ . \qquad (11)$$

Taking the logarithms

$$Np_l = 2\pi I_l + \sum_{j=1}^{n}\Theta(p_l, p_j)\ , \qquad (12)$$

where I_l must be an integer if n is odd and half integer if n is even. The form of $\Theta(p,q)$ being rather simple, the method of Yang and Yang [38] can be easily applied to prove that Eq. (16) has a unique solution with $I_l = l - (n+1)/2$, where $l = 1, \ldots, n$.

As the coordinate Bethe ansatz was constructed, see Eq. (1), the vertical down arrows were counted explicitly by n. Thus the ratio n/N is the proportion of down arrows in each row of the lattice. In other words, it is the probability to find a vertical arrow to be down. Due to the periodic boundary conditions applied standardly n is strictly equal for all rows [21]. In the limit $N \to \infty$ the momenta $p_1, \ldots, p_n$ become densely packed along a smooth curve C in the complex z plane. The curve C must be symmetrical with respect to the transformation $z \to z^*$ and will be determined later on. Let us denote the two ends of the curve C by Q_1 and Q_2. If we denote the number of p_i's lying between p and $p + dp$ by $N\rho(p)dp$, with $\rho(p)$ being the distribution function, then as the total number of p_i's is n, $\rho(p)$ must satisfy

$$\int_{Q_1}^{Q_2}\rho(p)dp = \frac{n}{N}\ . \qquad (13)$$

For a given value p of p_j, $I_j + (n+1)/2$ is the number of k_l's with $l < j$. Thus Eq. (16) becomes the well-known linear integral equation [38] for $\rho(p)$

$$2\pi\rho(p) + \int_{Q_1}^{Q_2}\frac{\partial\Theta(p,p')}{\partial p}\rho(p')dp' = 1\ . \qquad (14)$$

The value of

$$2\pi g(p) = 2\pi N\int_{Q_1}^{p}\rho(p')dp' \qquad (15)$$

is known at the end points due to Eq. (13). The curve of integration is defined [38] by those points z at which $\mathrm{Im}g = 0$. This equation is satisfied by any straight line symmetric to the imaginary axis of the complex z plane. Thus we obtain

$$Q_2 \equiv Q = q' + iq''\ ,$$
$$Q_1 \equiv -Q^* = -q' + iq''\ , \qquad (16)$$

with $q' \in [-\pi, +\pi]$ and $q'' \in [0, +\infty)$. The solution of Eq. (14) can be easily found:

$$\rho(p) = \frac{1}{2\pi}\left[1 + \frac{1-p_v}{2}\frac{\Delta_5 e^{ip}}{1-\Delta_5 e^{ip}}\right]\ . \qquad (17)$$

We recall that n represents the number of vertical down arrows on a row. Thus the vertical polarization is $p_v = 1-2n/N$. As it can be seen from Eq. (17) the distribution function has the same algebraic form for any Δ_5. This property is a direct consequence of the form of the kernel (see Appendix B) and not of its analytic properties.

The vertical polarization p_v can be also easily determined with the use of Eqs. (13) and (18):

$$p_v = 1 - 2q'/\{\pi + \mathrm{Im}[\ln(1-\Delta_5 e^{-q''}e^{iq'})]\}\ . \qquad (18)$$

Note that the value of the vertical polarization can be obtained directly also from Eq. (12) as we take the thermodynamic limit. The real part of this equation is exactly Eq. (18), while the imaginary part will give

$$\int_{-Q^*}^{+Q} \ln(1-\Delta_5 e^{ip})\rho(p)dp$$

$$= q'' + \frac{1-p_v}{2}\,\mathrm{Re}[\ln(1-\Delta_5 e^{-q''}e^{iq'})]\;, \quad (19)$$

This equation will be useful in the evaluation of the free energy. $\mathrm{Re}\ln z \equiv \ln|z|$, and for the imaginary part we used the obvious convention $\mathrm{Im}\ln z \equiv \arg z$.

For further considerations, we use the notations $x = \omega_1/\omega_5$ and $y = \omega_3/\omega_5$. As in the symmetric six-vertex case [22], the phase diagram can be conveniently drawn in the (x, y) plane. The free energies corresponding to the $\omega_2 = 0$ (five-vertex) case, determined from Eq. (1) are

$$f_L = \min_{p_v}\left\{\varepsilon_1 - k_B T\int_{-Q^*}^{+Q}\ln\left(\frac{1-\Delta_5 e^{ip}}{x/y - e^{ip}}\right)\rho(p)dp\right\}\;, \quad (20)$$

$$f_{M'} = \min_{p_v}\left\{\varepsilon_4 + k_B T(1-p_v)\ln y + k_B T\int_{-Q^*}^{+Q}\ln(x/y - e^{ip})\rho(k)dk\right\}\;,$$

the thermodynamic free energy being the smaller of the two (which will turn out to be f_L in all cases). Since the integrands are symmetric functions of $\mathrm{Re}p$ and antisymmetric for the transformation $p \to -p^*$, these integrands are real. In the thermodynamic limit both eigenvalues of Eq. (1) are growing exponentially, the larger dominating the smaller. However, with the use of Eq. (19) it can be shown, see also Appendix A and Ref. [37], that $f_L \le f_{M'}$.

III. THE FREE-FERMION SOLUTION

We will consider first the noninteracting limit, i.e., the $\Delta_5 = 0$ case, which was solved [36] already, but not thoroughly analyzed. The noninteracting case corresponds to $y = 1$. In this case, Eqs. (17), (18), and (20) simplify considerably, $f_L = f_{M'}$ with $\rho(k) = 1/2\pi$, $q' = \pi(1-p_v)/2$, and $q'' = 0$. The integral entering in the expression of the free energy is sensitively dependent on the value of x. For large values of x it is always negative, independently of Q. The free energy for $x \to \infty$ ($T \to 0$ limit) is

$$f_L = \varepsilon_1 + k_B T\,\frac{1-p_v}{2}\ln x\;. \quad (21)$$

To obtain the minimum value (i.e., ε_1), $p_v = 1$ must be considered. Thus the system at $T = 0$ is in a completely polarized state. To depart from this ferroelectric state, the obvious condition $1 + x^2 - 2x\cos k \ge 1$ is required. The equality defines the transition for $p_v = 1$. A remarkable feature of this phase transition, as it was noted already by Kasteleyn [2], is that up to the transition point the system shows a perfect ordering, i.e., the transition is a second-order phase transition of a rather unusual kind. In the usual case, e.g., at the Curie point of a ferromagnet, the order parameter vanishes on both sides of the transition; here, on the contrary, it is maximal. The second-order phase transition occurs at $x = 2$, a relation which defines the critical transition temperature $k_B T_c = (\varepsilon_4 - \varepsilon_1)/\ln 2$. This result was also obtained by Wu [36]. It should be noted that a frozen-in ferroelectric state is obtained in this $\Delta_5 = 0$ case which is distinct from that for $\Delta_5 > 1$ indicated above.

The free energy is ε_1 for $x > 2$ and is equal to

$$f_L = \varepsilon_1 + \frac{k_B T}{2\pi}\int_0^{q'}\ln(1 + x^2 - 2x\cos k)dk \quad (22)$$

for $1 \le x \le 2$. Here, $q' = \cos^{-1}(x/2)$ which, due to $q' = \pi(1-p_v)/2$, defines also the polarization per vertex. The form of the free energy given in Eq. (22) is identical to that obtained by Wu [36]. It is found that the vertical polarization does not vanish in zero field. p_v is a smooth function of x, being equal to unity for $x = 2$ ($T = T_c$), and reaches the $p_v = 1/3$ value at $x = 1$ ($T \to \infty$). This is in contradiction with the symmetric six-vertex results, where at infinite temperature all vertices are equally probable ($p_v = 0$). In the present case, however, we have $n_1 = 1/3$ and $n_3 = n_4 = n_5 = n_6 = 1/6$. The internal energy is a continuous function of x, thus also of T. The specific heat $c = 0$ for $x > 2$, i.e., $T < T_c$. Near the transition

$$c[x \to 2_{(-)}] = \frac{\sqrt{2}\ln^2 2}{\pi\sqrt{1 - x/2}}\;, \quad (23)$$

that is

$$c[T \to T_{c(+)}] = \frac{\sqrt{2}T_c\ln^2 2}{\pi\sqrt{\varepsilon_4 - \varepsilon_1}\sqrt{T - T_c}}\;. \quad (24)$$

The critical exponent α is thus $\alpha = 1/2$.

The $x \to 1$ limit has a major significance because it corresponds to $T \to \infty$. The specific heat smoothly decreases as x decreases, vanishing for $x = 1$ as

$$c[x \to 1_{(+)}] = (x-1)^2\frac{5 + \pi\sqrt{3}}{3\pi\sqrt{2}}\;. \quad (25)$$

The same behavior is obtained in the $x \le 1$ variation range. In this case the free energy is given by

$$f_M = \varepsilon_4 + \frac{k_B T}{2\pi}\int_0^{q'}\ln(1 + x^2 - 2x\cos k)dk\;, \quad (26)$$

This means that the specific heat approaches zero at infinite temperature in both limits as

$$c(T \to \infty) = q\frac{(\varepsilon_4 - \varepsilon_1)^2}{T^2}\;, \quad (27)$$

where $q = (5 + \pi\sqrt{3})/3\pi\sqrt{2}$. The entropy in the same limit is equal to the known value [29]

$$S(T \to \infty) \equiv S_\infty = \frac{Cl_2(\pi/3)}{\pi} \simeq 0.323\;, \quad (28)$$

where $Cl_2(z) = -\int_0^z \ln[2\sin(x/2)]dx$ is Clausen's integral [39]. This value is considerably smaller than the entropy density of the six-vertex model, where [21] $S_6 = 3[\ln 2 - (1/2)\ln 3] \simeq 0.431$. In the same limit, the free energy behaves as

$$f(T \to \infty) = \text{const} - TS_\infty \,. \tag{29}$$

At this point, we must mention that the free energy can be written in a compact form (even in the $\Delta_5 \neq 0$ case) using Clausen's integral, or as a series of dilogarithm functions [40].

IV. THE PHASE DIAGRAM

Hereafter we study the analytic properties and the phase diagram of the free energy f_L given in Eq. (20).

Let us first study the ferroelectric transition, which occurring at $p_v = 1$ is characterized by a complete polarization. The curve at which this transition occurs can be easily obtained [32, 37] if we recall that $p_v \to 1$ corresponds to $n \to 0$. Directly from Eq. (1) by setting $k_1, \ldots, k_n = 0$ the transition curves are obtained to be

$$x = \begin{cases} y - 1/y & \text{for } x < y \\ y + 1 & \text{for } x > y, \end{cases} \tag{30}$$

corresponding to curves a and b of Fig. 1, respectively.

The analytic properties of the free energy close to these transition curves can be studied by transforming f_L from Eq. (20) to

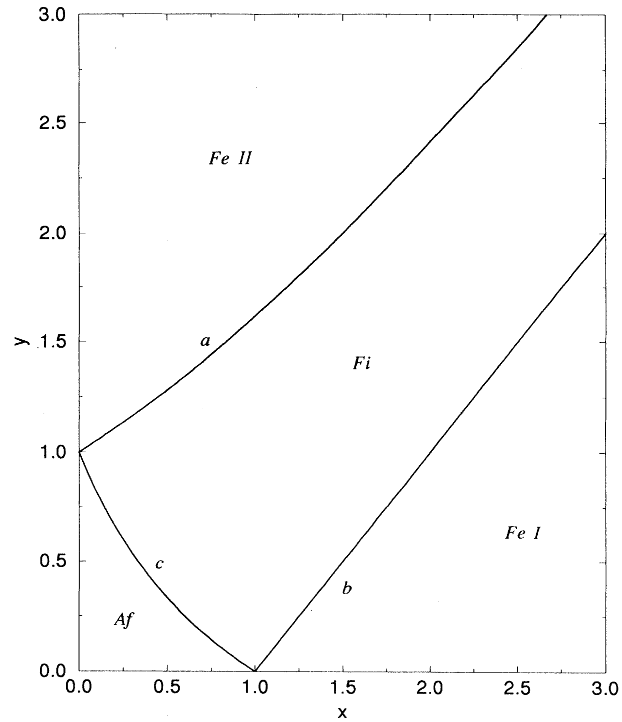

FIG. 1. The phase diagram of the five-vertex model in zero external field, in terms of the Boltzmann weights $x = \omega_1/\omega_5$ and $y = \omega_3/\omega_5$ ($\omega_2 = 0$, $\omega_3 = \omega_4$, and $\omega_5 = \omega_6$). All curves represent (second-order) continuous transitions. Fe stands for a ferroelectric, Fi for a ferrielectric, and Af for an antiferroelectric phase. The $x = y = 1$ point corresponds to infinite temperature, while any point satisfying $x/y = 0$ or $y/x = 0$ corresponds to $T = 0$.

$$f_L = \varepsilon_1 - k_B T \int_{-q'}^{+q'} \text{Re}\ln\frac{1 - \Delta_5 e^{-q''} e^{ip'}}{x/y - e^{-q''} e^{ip'}} \text{Re}\rho(p' + iq'')dp' + k_B T \int_{-q'}^{+q'} \left\{ \text{Im}[\ln(1 - \Delta_5 e^{-q''} e^{ip'})] - \text{Im}\left[\ln\left(\frac{x}{y} - e^{-q''} e^{ip'}\right)\right]\right\} \text{Im}\rho(p' + iq'')dp' \,, \tag{31}$$

where the $p = p' + ip''$ notation was used. Other combinations of functions will give an integrand in Eq. (31) which is an even function of p'. Thus their integral over a symmetric domain vanishes.

The vertical polarization obtained in Eq. (18) equals unity for any q'' and Δ_5 if $q' \to 0$. Clearly, the integrals from Eq. (31) are vanishing in this limit for $x > y$. In the opposite case, i.e., $y > x$, care should be given to eliminate the occurring divergences. Let us analyze the two cases separately.

In the $x > y$ situation we can borrow the computing procedure from the noninteracting case. In particular we study the ferroelectric transition (line b in Fig. 1). The latter is obtained taking the $q' \to 0$ limit. In order to obtain the minimum value of f_L in the $q' \to 0$ limit we must require the first integral to be maximal and the second one minimal. Thus the first integrand of Eq. (31) must be positive. This implies that the condition

$$\frac{1 - 2\Delta_5 e^{-q''}\cos p' + \Delta_5^2 e^{-2q''}}{(x/y)^2 - 2(x/y)e^{-q''}\cos p' + e^{-2q''}} \geq 1 \tag{32}$$

will determine the variation range of p'. In Eq. (32) the equality defines the maximum value of p', i.e. the integration limit, for which we obtain

$$q' = \arccos\left(\frac{(x/y)^2 + (1 - \Delta_5^2)e^{-2q''} - 1}{2(x/y - \Delta_5)e^{-q''}}\right) \tag{33}$$

for any q''. The value of the latter is determined by minimizing the second integral from Eq. (31), obtaining $q'' \to 0$. Thus the analytic form of the vertical polarization is governed by Eqs. (18) and (33). The minimum of f_L for any $x > y$ and $q' \to 0$ is

$$f_L = \varepsilon_1 - \frac{k_B T}{2\pi} \int_0^{+q'} \ln\left[\frac{1}{x^2}\left(y^2 + \frac{1 - 2y^2 + 2xy\cos p'}{x^2 + y^2 - 2xy\cos p'}\right)\right] dp' , \tag{34}$$

with q' given in Eq. (33). Equating q' to zero gives the transition line $x = y + 1$ from Eqs. (30). To the right of this line the free energy is ε_1. That is, in the region Fe I of Fig. 1, the system is an ideal ferroelectric. The lowest energy state is one where all vertices are of type 1. This ferroelectric phase remains stable on the whole region Fe I of Fig. 1, even for low values of y, where $\Delta_5 < -1$.

In order to see what type of transition occurs, we calculate the thermodynamic quantities. We obtain that the internal energy is a continuous function on the whole transition line, while the specific heat near the transition behaves as

$$c(x,y) = \frac{(\varepsilon_5 - \varepsilon_1)^2}{T^2} x^2 \frac{\partial q'}{\partial x}\left[\frac{\partial F_L(x,y,p')}{\partial x}\right]\Bigg|_{p'=q'} + \frac{(\varepsilon_5 - \varepsilon_1)(\varepsilon_5 - \varepsilon_4)}{T^2} xy \frac{\partial q'}{\partial x}\left[\frac{\partial F_L(x,y,p')}{\partial y}\right]\Bigg|_{p'=q'}$$
$$+ \frac{(\varepsilon_5 - \varepsilon_1)(\varepsilon_5 - \varepsilon_4)}{T^2} xy \frac{\partial q'}{\partial y}\left[\frac{\partial F_L(x,y,p')}{\partial x}\right]\Bigg|_{p'=q'} + \frac{(\varepsilon_5 - \varepsilon_4)^2}{T^2} y^2 \frac{\partial q'}{\partial y}\left[\frac{\partial F_L(x,y,p')}{\partial y}\right]\Bigg|_{p'=q'} + \text{const.} \tag{35}$$

$F_L(x,y,p')$ is the integrand from Eq. (34). Using the analytic form of q' from Eq. (33), we see that the $\partial q'/\partial x(\ y)$ term introduces a square-root divergence approaching the $x = y + 1$ transition line. Thus the specific heat behaves like $c[x \to (y+1)_{(-)}] \sim [1 - x/(y+1)]^{-1/2}$, in terms of temperature $c[T \to T_{c(+)}] \sim [T - T_c]^{-1/2}$. This means that curve b of Fig. 1 represents a second-order phase transition, with critical exponent $\alpha = 1/2$ (as in the noninteracting case).

In the $x < y$ situation, as mentioned previously, care should be given to the divergent integrand. We write the free energy with the use of Eq. (19) as

$$f_L = \varepsilon_1 - k_B T\left[q'' + \frac{1}{\pi}\sum_{n=1}^{\infty}\frac{1}{n^2}\left(\frac{y}{x}e^{-q''}\right)^n \sin(nq')\right] - k_B T\frac{1-p_v}{2}\,\text{Re}[\ln(1 - \Delta_5 e^{-q''}e^{iq'})] - \ln\frac{x}{y}$$
$$+ \frac{1}{\pi}\ln\left(1 - \frac{y}{\Delta_5 x}\right)\text{Im}\left[\ln\frac{\Delta_5 e^{-q''}e^{iq'} - 1}{\Delta_5\frac{x}{y} - 1}\right]$$
$$+ \frac{1}{\pi}\sum_{n=1}^{\infty}\frac{1}{n^2}\left\{\text{Re}\left[\ln\frac{\Delta_5 e^{-q''}e^{iq'} - 1}{\Delta_5\frac{x}{y} - 1}\right]\right\}^n \sin\left\{n\,\text{Im}\left[\ln\frac{\Delta_5 e^{-q''}e^{iq'} - 1}{\Delta_5\frac{x}{y} - 1}\right]\right\} . \tag{36}$$

For $p_v \to 1$ the minimum value of the free energy from Eq. (36) is obtained for $e^{-q''} = x/y$, the value for which the first summation is maximal. Considering also $p_v \to 1$ and $q' \to 0$, Eq. (36) reduces to

$$f_L = \varepsilon_4 - k_B T\frac{1-p_v}{2}\ln\Delta_5 . \tag{37}$$

As it can be seen, the second ferroelectric transition occurs at $\Delta_5 = 1$, i.e., at the $x = y - 1/y$ curve, see Eqs. (30). The system is in a frozen-in state in the region Fe II of Fig. 1: the lowest energy state is one in which all vertices are 4 or 3.

Equation (37) can be taken as the first two terms in an $1 - p_v$ expansion of the free energy near the transition. The following contribution is obtained directly from Eq. (36). Thus the free energy close to the transition curve becomes

$$f_L = \varepsilon_4 - k_B T\frac{1-p_v}{2}\ln\Delta_5$$
$$- k_B T\frac{\pi^2}{2}y^3(y^2 - 1)\left(\frac{1-p_v}{2}\right)^3 . \tag{38}$$

Note that the second term of this expansion is positive due to the fact that $\Delta_5 < 1$, while the third term is negative, as we have $y > 1$. From Eq. (38) the vertical polarization, near the transition, can be expressed as

$$\frac{1-p_v}{2} = \sqrt{\frac{2}{3\pi^2}\frac{\ln(1/\Delta_5)}{y^3(y^2-1)}} . \tag{39}$$

It can be seen, from Eq. (39), that indeed $\Delta_5 = 1$ implies $p_v = 1$. The free energy from Eq. (38) with the use of Eq. (39) becomes

$$f_L = \varepsilon_4 + k_B T(\tfrac{2}{3})^{3/2}\frac{\ln^{3/2}(1/\Delta_5)}{\pi\sqrt{y^3(y^2-1)}} . \tag{40}$$

Thus the free energy varies like $f_L[T \to T_{c(+)}] \sim [T - T_c]^{3/2}$, which implies for the internal energy $u[T \to T_{c(+)}] \sim [T - T_c]^{1/2}$. Thus the internal energy is a continuous function at the transition. The specific heat is zero to the left of the transition curve. But from the right it diverges like $c[T \to T_{c(+)}] \sim [T - T_c]^{-1/2}$. The a transition curve represents another second-order phase transition, again with critical exponent $\alpha = 1/2$.

Between the a and b transition curves the vertical and horizontal polarizations are smooth functions of x and y.

Since this domain, region Fi of Fig. 1, which is delimited by the a, b, and c transition curves, has a nonvanishing polarization per vertex, it will correspond to a ferrielectric phase. Approaching both curves a and b the vertical polarization tends to unity, being equal to unity on the whole transition curves.

In the $\Delta_5 < -1$ region an antiferroelectric phase is expected. As in the previous case, we must take care of the divergences which occur in the expression of the free energy f_L, Eq. (20) in this limit. In doing this we perform an integral variable change as in Ref. [37], or in Nolden's thesis [42]. The form of the kernel from Eq. (9) suggests a transformation $p \to p(\alpha)$ which reduce it to $\Theta(\alpha,\beta) = \alpha - \beta$. Under the transformation (p,q) to (α,β) the integration path C is mapped in a curve C' and the end points Q and $-Q^*$ to $+a+ib$ and $-a+ib$. Since the integration path is a straight line, we introduce the new variables $\alpha = u+ib$ and $\beta = v+ib$ to obtain integrals running on the real axis. In these new variables $\Theta(\alpha-\beta) = \Theta(u-v) = u-v$. The distribution function from Eq. (17) becomes

$$R(u,b) = -\frac{1-p_v}{2} + \frac{e^{-b}e^{iu}}{e^{-b}e^{iu}-1}\,, \tag{41}$$

while the vertical polarization is

$$\frac{1-p_v}{2} = \frac{\mathrm{Im}[\ln(e^{-b}e^{iu}-1)]}{\pi+a}\,. \tag{42}$$

The free enregy f_L from Eq. (20) in the transformed variables becomes

$$f_L = \varepsilon_1 - \frac{k_BT}{2\pi}\int_{-a}^{+a} R(u,b)\left[iu - b - \ln\left(\frac{x}{y} - \frac{1-e^{-b}e^{iu}}{\Delta_5}\right)\right]du\,. \tag{43}$$

To simplify the expression of the free energy we transform Eq. (12) into the new variables and perform the thermodynamic limit. The real part of the equation so obtained is exactly Eq. (42) while the imaginary part is

$$\mathrm{Re}\left[\ln\frac{1-e^{-b}e^{ia}}{\Delta_5}\right] + \frac{a}{\pi}\mathrm{Re}[\ln(e^{-b}e^{ia}-1)] + \frac{ab}{\pi} + \frac{1}{\pi}\sum_{n=1}^{\infty}\frac{e^{nb}}{n^2}\sin(na) = 0\,. \tag{44}$$

As it can be seen from Eq. (42) an antiferroelectric phase is reached for $a=\pi$, which corresponds to $q'=\pi$ in Eq. (18). To obtain the transition curve we evaluate the free energy in the limit $p_v \to 0$. Performing the integral in Eq. (43) [40] and using Eq. (44) we obtain

$$f_L = \varepsilon_1 + k_BT\left\{\ln x + b + \ln y - 2\sum_{n=1}^{\infty}\frac{1}{n^2}\left(\frac{y^2(1+e^{-b})}{1-y^2}\right)^n \sin[n\arctan(e^{-b}\sin a, e^{-b}\cos a - 1)]|_{a\to\pi}\right\}, \tag{45}$$

where $\arctan(x,y)$ is the *two-argument* arctan function [40], i.e., $\arctan(x,y) = \arctan(y/x) \pm \pi$. The free energy for $p_v = 0$ is obtained from Eq. (45) to be

$$f_L = \varepsilon_5 + k_BT(b + \ln y)\,, \tag{46}$$

where b must be determined from Eq. (44) in the same limit, obtaining

$$\ln\frac{(1+e^{-b})^2}{e^{-b}|\Delta_5|} = 0\,. \tag{47}$$

The minimum of the free energy is obtained for $b = -\ln y$. This means that the antiferroelectric phase is built up only with vertices five and six. Thus the ordered antiferroelectric phase is in frozen-in state. This is a very interesting result, as no other vertex model exhibit a frozen-in antiferroelectric phase. In order to understand this result, we recall the definitions of the vertical and horizontal polarizations, which are $p_v = n_1 - n_3 + n_4$ and $p_h = n_1 + n_3 - n_4$, respectively. It can be seen that an antiferroelectric phase can be realized only if $n_1 = 0$ and $n_3 = n_4$. However, these conditions represent the $\Delta_6 \to -\infty$ $(T \to 0)$ limit of the symmetric six-vertex model [22], which is frozen in ε_5 and ε_6.

Combining Eqs. (46) and (47) the transition curve becomes

$$x = \frac{1-y}{1+y}\,, \tag{48}$$

which is curve c from Fig. 1. Below this curve the lowest-energy state is one in which all vertices are 5 and 6. The free energy close to the transition can be obtained from Eq. (45)

$$f_L = \varepsilon_5 - k_BT\frac{p_v}{2}\ln\frac{1-y}{x(1+y)} - k_BT\frac{(p_v\pi)^3}{3}F(y)\,, \tag{49}$$

where $F(y)$ is a function dependent only on y; see Ref. [43]. Note that the second term of Eq. (49) is positive as x approaches the transition curve from above. The vertical polarization from Eq. (49) can be obtained to be

$$p_v = \sqrt{\frac{\ln[(1-y)/x(1+y)]}{2\pi^3F(y)}}\,. \tag{50}$$

It can be seen that Eq. (50), indeed implies $p_v = 0$ at the transition curve. The free energy from Eq. (49) with the use of Eq. (50) becomes

$$f_L = \varepsilon_5 + k_B T \frac{5}{24\pi^{3/2}} \frac{\ln^{3/2}[(1-y)/x(1+y)]}{\sqrt{F(y)}}. \qquad (51)$$

Thus the free energy varies like $f_L[T \to T_{c(+)}] \sim [T - T_c]^{3/2}$, which implies for the internal energy $u[T \to T_{c(+)}] \sim [T - T_c]^{1/2}$. Thus the internal energy is a continuous function at the transition. The specific heat is zero below the transition curve. But, from above it diverges like $c[T \to T_{c(+)}] \sim [T - T_c]^{-1/2}$. The c transition curve represents once more a second-order phase transition, with critical exponent $\alpha = 1/2$. Thus all the ordered phases which appear in the five-vertex model are in a frozen-in state, and all transitions are second-order, with $\alpha = 1/2$.

Closing, we mention that the frozen-in antiferroelectric phase boundary obtained in Eq. (28) can be obtained from an SOS model point of view, as it follows. The elementary excitation of the antiferroelectric groundstate is a step with the properties of a SOS phase boundary. The step may go upward or downward and to the right. Each step to the right will have a normalized Boltzmann weight x and each step moving on the vertical axis will have y. The partition function of an elementary step will be

$$\left[x\left(\sum_{Y=1}^{\infty} y^Y - 1\right)\right]^N = \left(x\frac{1+y}{1-y}\right)^N, \qquad (52)$$

with N being the horizontal width. These steps will occur as $x(1+y)/(1-y) > 1$. Thus the phase boundary of the antiferroelectric phase will be given by Eq. (28).

V. CONCLUSIONS

We have shown that the Bethe ansatz provides exact eigenvalues for the five-vertex model. As the analysis of the eigenvalues and eigenfunction demonstrates, the model turns out to be easily integrable due to the presence of a degenerate kernel. The five-vertex model can be connected to a specific limit of the asymmetric six-vertex model, where both the horizontal and vertical external fields and the vertex energies have to approach infinity simultaneously. This approach makes the five-vertex limit difficult to handle and infinitely large additive constants to appear. Therefore we obtained a direct solution of the five-vertex model by applying the Bethe ansatz afresh. Doing this, we were also able to study simply the effect of an external field on the five-vertex model (i.e., to determine its phase diagram in a field) and to calculate the correlations along a row, results which will be the subject of a future publication.

The phase diagram obtained in the thermodynamic limit contains only continuous transitions of second order. Several aspects of the phase diagram are unusual. Even the second-order transitions are of unusual type, because the order parameter is equal to unity on both sides of the transition, instead of vanishing as in the Curie point of a ferromagnet. The model exhibits an antiferroelectric phase built up only with vertices 5 and 6. Thus, even the ordered antiferroelectric phase is in a frozen-in state. This is interesting, since no other vertex model is known to have a frozen-in antiferroelectric phase. The model also exhibits two frozen-in ferroelectric phases, which are suitable to describe, from the point of view of Garrod, Levi, and Touzani's theory [29], perfectly smooth surfaces of simple cubic crystals.

ACKNOWLEDGMENTS

The authors have benefited from continuing and enlightening discussions with Professor Erio Tosatti, without whom this work would not have been accomplished. Most of this work was performed while two of the authors (M.G. and A.C.L.) were at the SISSA, Trieste.

APPENDIX A: CONNECTION BETWEEN THE ASYMMETRIC SIX- AND FIVE-VERTEX MODELS

In the asymmetric six-vertex model the following four new variables are defined [32, 37, 42]:

$$\eta = \sqrt{\frac{\omega_1\omega_2}{\omega_3\omega_4}} \equiv e^{\beta\delta}\ , \ \xi = \frac{\omega_5\omega_6}{\sqrt{\omega_1\omega_2\omega_3\omega_4}} \equiv e^{2\beta\epsilon}\ , \qquad (A1)$$

and

$$H = \sqrt{\frac{\omega_1\omega_3}{\omega_2\omega_4}} \equiv e^{2\beta h}\ , \ V = \sqrt{\frac{\omega_1\omega_4}{\omega_2\omega_3}} \equiv e^{2\beta v}\ , \qquad (A2)$$

where h and v are the horizontal and vertical field components. The interaction constant is introduced as

$$\Delta_6 = \frac{1}{2}\left(\eta + \frac{1}{\eta} - \xi\right). \qquad (A3)$$

Using these new variables, as mentioned in Sec. II, the model is symmetric with respect to reversing all arrows and the external electric field. The textbook solution of the asymmetric six-vertex model runs as follows. The free energy from Eq. (2), with the transformed variables defined in Eqs. (A1), and (A2) is

$$f(\eta,\xi,h,v) = f(\eta,\xi,h) - vp_v - \frac{k_BT}{4}\ln(\omega_1\omega_2\omega_3\omega_4)\ , \qquad (A4)$$

where $p_v = 1 - 2n/N$ is the vertical polarization and $f(\eta,\xi,h) = -k_BT/N \ln\Lambda(n)$, with

$$\Lambda(n) = (\eta H)^{N/2}\prod_{i=1}^{n}\left[\eta^{-1} - \frac{\eta}{1-\eta H z_i}\right] + (\eta H)^{-N/2}\prod_{i=1}^{n}\left[\eta - \frac{\eta}{1-(\eta H z_i)^{-1}}\right] \qquad (A5)$$

of the well-known form [21, 32, 37]. Since the model is symmetric with respect to reversing all arrows and the external field, it is controlled by four independent variables. These are obtained by imposing [32, 37] $\omega_5 = \omega_6$ [34] and $\omega_1\omega_2\omega_3\omega_4 = 1$. In these conditions the six allowed vertices are obtained as

$$\begin{aligned}\varepsilon_1 &= -\frac{1}{2}\delta - h - v, \quad \varepsilon_2 = -\frac{1}{2}\delta + h + v,\\ \varepsilon_3 &= +\frac{1}{2}\delta - h + v, \quad \varepsilon_4 = +\frac{1}{2}\delta + h - v,\\ \varepsilon_5 &= -\epsilon, \quad \varepsilon_6 = -\epsilon\end{aligned} \tag{A6}$$

and the free energy of the asymmetric six-vertex model can be given in terms of the *rapidity* ϕ, defined as

$$e^{-i\phi} = \begin{cases} \frac{1+e^{\lambda}\eta}{e^{\lambda}+\eta} & \text{for} \Delta_6 < -1, \Delta_6 = -\cosh\lambda, \lambda > 0 \\ \frac{1+e^{i\mu}\eta}{e^{i\mu}+\eta} & \text{for } |\Delta_6| < 1, \Delta_6 = -\cos\mu, 0 < \mu < \pi \\ \frac{e^{\nu}\eta-1}{\eta-e^{\nu}} & \text{for } \Delta_6 > 1, \Delta_6 = \cosh\nu, \nu > 0. \end{cases} \tag{A7}$$

We note that the parametrization from Eqs. (A7) are for the $\eta \leq 1$ case. For the opposite case $\eta \geq 1$, analyzed in Refs. [32, 37], the $\phi \leftrightarrow -\phi$ change should be performed. Combining Eqs. (A7) with Eqs. (A1) and (A2) the products of the Boltzmann weights can be expressed as [32]

$$\omega_1\omega_2 = \begin{cases} \sinh^2\frac{1}{2}(\lambda-\phi), \Delta_6 < -1 \\ \sin^2\frac{1}{2}(\mu-\phi), |\Delta_6| \leq 1 \\ \sinh^2\frac{1}{2}(\nu-\phi), \Delta_6 > 1, \end{cases} \tag{A8}$$

$$\omega_3\omega_4 = \begin{cases} \sinh^2\frac{1}{2}(\lambda+\phi), \Delta_6 < -1 \\ \sin^2\frac{1}{2}(\mu+\phi), |\Delta_6| \leq 1 \\ \sinh^2\frac{1}{2}(\nu+\phi), \Delta_6 > 1, \end{cases} \tag{A9}$$

and

$$\omega_5\omega_6 = \begin{cases} \sinh^2\lambda, \Delta_6 < -1 \\ \sin^2\mu, |\Delta_6| \leq 1 \\ \sinh^2\nu, \Delta_6 > 1. \end{cases} \tag{A10}$$

Naively, one might think to obtain the five-vertex model by simply letting $\omega_2 = 0$ in the above equations. But it can be seen immediately that for any $\omega_1 = a$ finite and $\omega_2 = 0$, Eq. (A8) implies $\lambda = \phi$ (respectively, $\mu = \phi$ or $\nu = \phi$) in the three cases. Hence Eqs. (A9) and (A10) yield $\omega_3\omega_4 = \omega_5\omega_6$, which is nothing other than the free fermion condition [41].

As it can be seen from Eqs. (A1)–(A3), in order to obtain other than the non-interacting case the following limits $\eta \to 0$, $\xi \to \infty$, $H \to V \to \infty$, and $\Delta_6 \to \pm\infty$ must be taken, in a way that the products $\eta\xi$, ηH and the ratios ξ/H, Δ_6/H are finite. The manipulation is rather delicate, however, since these limits are obviously related. We find, using the notation of Sec. II,

$$\eta|_{H\to\infty} = \frac{x}{Hy}, \quad \xi|_{H\to\infty} = \frac{H}{xy}, \tag{A11}$$

$$\Delta_6|_{H\to\infty} = \frac{H}{2}\Delta_5.$$

Thus the original six vertex energies ($\varepsilon_i^{\{6\}}$) from Eqs. (A6) are related to the five vertex ones ($\varepsilon_1^{\{5\}}$, $\varepsilon_3^{\{5\}} = \varepsilon_4^{\{5\}}$, and $\varepsilon_5^{\{5\}} = \varepsilon_6^{\{5\}}$) in the $h \to \infty$ as

$$\begin{aligned}\varepsilon_1^{\{6\}} &= \frac{1}{2}(\varepsilon_1^{\{5\}} - \varepsilon_3^{\{5\}}) - h,\\ \varepsilon_2^{\{6\}} &= \frac{1}{2}(\varepsilon_1^{\{5\}} - \varepsilon_3^{\{5\}}) + 3h,\\ \varepsilon_3^{\{6\}} &= \frac{1}{2}(\varepsilon_3^{\{5\}} - \varepsilon_1^{\{5\}}) - h,\\ \varepsilon_4^{\{6\}} &= \frac{1}{2}(\varepsilon_3^{\{5\}} - \varepsilon_1^{\{5\}}) - h,\\ \varepsilon_5^{\{6\}} &= \frac{1}{2}(2\varepsilon_5^{\{5\}} - \varepsilon_1^{\{5\}} - \varepsilon_3^{\{5\}}) - h,\\ \varepsilon_6^{\{6\}} &= \frac{1}{2}(2\varepsilon_5^{\{5\}} - \varepsilon_1^{\{5\}} - \varepsilon_3^{\{5\}}) - h\,.\end{aligned} \tag{A12}$$

To handle the free energy $f(\eta, \xi, h)$ given in Eqs. (A4) and (A5) in the limit of Eqs. (A11) is rather difficult. However, it can be shown that up to an additive (infinitely large) constant the expressions of f_L and $f_{M'}$ are obtained. It is known [37] that $f_L \leq f_{M'}$ always.

In the following we present one of the few, relatively tractable limits of the asymmetric six-vertex results, namely the derivation of the transition curves. In the limit of Eqs. (A11), the two transition curves which define the phase boundaries of ferroelectric phases, Eqs. (30) of Sec. IV can be obtained without major difficulty from Eqs. (355) of Ref. [21]. Concerning the antiferroelectric phase, its transition curve is given by [42]

$$\ln H = -q'' - 2\sum_{n=1}^{\infty}\frac{(-1)^n}{n}\frac{\sinh q''n}{\cosh\lambda n}\,, \tag{A13}$$

where q'' is an integration limit similar to that defined in Eq. (16) and λ was defined in Eqs. (A7). In the $H \to \infty$ limit we obtain

$$e^{q''} = H\frac{1-y^2}{x}, \; e^{\lambda} = H\frac{1-y^2}{xy}\,, \tag{A14}$$

which together with Eq. (12) gives Eq. (48) of Sec. IV.

APPENDIX B: ANALYTIC PROPERTIES OF THE KERNEL

Let us study the analytic properties of the $\Theta(p,q)$ function defined in Eq. (9). Notice that $\mathrm{Re}\Theta(-p^*,-q^*) = -\mathrm{Re}\Theta(p,q) = \mathrm{Re}\Theta(q,p)$ and $\mathrm{Re}\Theta(0,0) = 0$, while $\mathrm{Im}\Theta(-p^*,-q^*) = \mathrm{Im}\Theta(p,q)$ and $\mathrm{Im}\Theta(0,0) = 0$. Concerning its definition interval, $\Theta(p,q)$ is a single-valued analytic function of Δ_5, p, and q if the real parts of the two latter variables lie in the open interval of the variation range of the k_i's, which is the following

$$\begin{aligned}&-(\pi-\nu) < k_i < \pi - \nu \quad \text{for } |\Delta_5 e^r| \geq 1,\\ &-(\pi-\mu) < k_i < \pi - \mu \quad \text{for } -1 < \Delta_5 e^r < 1\,.\end{aligned} \tag{B1}$$

The parametrization which is defined by the form of $\Theta(p,q)$, corresponding to Eq. (B1), is

$$\begin{aligned}\Delta_5 e^r &= -\sec\nu, \quad 0 \leq \nu < \pi/2\\ \Delta_5 e^r &= -\cos\mu, 0 < \mu < \pi\,.\end{aligned} \tag{B2}$$

These conditions are very important, because they define uniquely the branch of the *ln* function in Eq. (9).

Under the conditions of the $|\Delta_5 e^r| \geq 1$ case, see Eqs. (B1), we have

$$-|\pi - 2\nu| < \mathrm{Re}\Theta(p,q) < |\pi - 2\nu| \,, \tag{B3}$$

and $\mathrm{Re}\Theta(p,q)$ has a discontinuity at those p and q values at which its denominator vanishes. On the other hand, if $-1 < \Delta_5 e^r < 1$, then

$$-|\pi - 2\mu| < \mathrm{Re}\Theta(p,q) < |\pi - 2\mu| \,, \tag{B4}$$

and there are no singularities. This behavior of the $\mathrm{Re}\Theta(p,q)$ function in the intervals $|\Delta_5 e^r| \geq 1$ and $-1 < \Delta_5 e^r < 1$ is identical [38] to the behavior of the symmetric six-vertex kernel in the intervals $\Delta_6 \leq -1$ and $-1 < \Delta_6 < 1$. The Δ_6 notation is self-explanatory. On the other hand, $\mathrm{Im}\Theta(p,q)$ behaves as a real logarithmic function in both cases.

By direct differentiation of Eq. (9) it can be seen that, e.g.,

$$\frac{\partial\Theta(p,q)}{\partial p} = -\frac{\Delta_5 e^{ip}}{1 - \Delta_5 e^{ip}} \,, \tag{B5}$$

that is, the kernel of the five-vertex model is degenerate.

---

* Present address.

[1] L. Onsager, Phys. Rev. **65**, 117 (1944); in *Critical Phenomena in Alloys, Magnets and Superconductors*, edited by R. E. Mills, E. Ascher, and R. I. Jaffe (McGraw-Hill, New York, 1971).

[2] P. W. Kasteleyn, Physica **21**, 1209 (1961), J. Math. Phys. **4**, 287 (1963).

[3] M. E. Fisher, Phys. Rev. **124**, 1664 (1961).

[4] The spherical model [T. H. Berlin and M. Kac, Phys. Rev. **86**, 821 (1952)] is distinct from the other exactly solvable models as it allows an exact solution in any dimension, but it has the nonphysical feature that it introduces interactions between spins infinitely far apart. Due to this, its solution differs in nature from that of other models.

[5] R. J. Baxter and I. G. Enting, J. Phys. A **9**, L149 (1976).

[6] G. E. Andrews, R. J. Baxter, and P. J. Forrester, J. Stat. Phys. **35**, 193 (1984).

[7] R. J. Baxter and F. Y. Wu, Phys. Rev. Lett. **31**, 1294 (1973); Aust. J. Phys. **27**, 357 (1974).

[8] R. J. Baxter, J. Phys. A **13**, L61 (1980); J. Stat. Phys. **26**, 427 (1981); R. J. Baxter and P. A. Pearce, J. Phys. A **15**, 897 (1982).

[9] R. J. Baxter, Phys. Rev. Lett. **26**, 832 (1971); Ann. Phys. (N.Y.) **70**, 193 (1972); **70**, 229 (1972); **76**, 1 (1973); **76**, 25 (1973); **76**, 48 (1973).

[10] R. J. Baxter, J. Phys. C **6**, L445 (1973); R. J. Baxter, S. B. Kellhand, and Y. F. Wu, J. Phys. A **9**, 397 (1976); R. J. Baxter, Proc. R. Soc. London Ser. A **383**, 43 (1982).

[11] H. N. V. Temperley and E. H. Lieb, Proc. R. Soc. London Ser. A **322**, 251 (1971).

[12] E. H. Lieb, Phys. Rev. **162**, 162 (1967); Phys. Rev. Lett. **18**, 1046 (1967); **19**, 108 (1967).

[13] J. D. Johnson, S. Krinsky, and B. McCoy, Phys. Rev. A **8**, 2526 (1973).

[14] C. Destri, H. J. van Vega, and H. J. Giacomini, J. Stat. Phys. **56**, 291 (1989).

[15] R. J. Baxter, Physica D **18**, 321 (1986).

[16] Note that in three dimensions, one model, Zamolodchikov's model, is known to be exactly solvable. Its solution was initially conjectured by Zamolodchikov himself (A. B. Zamolodchikov, Zh. Eksp. Teor. Fiz. **79**, 641 (1980) [Sov. Phys.—JETP **52**, 325 (1980)] and Commun. Math. Phys. **79**, 489 (1981)) and verified to be exact by Baxter [R. J. Baxter, Phys. Rev. Lett. **53**, 1795 (1984)]; see also Ref. [15].

[17] R. J. Baxter, Phys. Rev. Lett. **53**, 1795 (1984).

[18] M. Suzuki and M. E. Fisher, J. Math. Phys. **12**, 235 (1970).

[19] F. Y. Wu, Phys. Rev. Lett. **22**, 1174 (1969); **24**, 1476 (1970).

[20] J. C. Slater, J. Chem. Phys. **9**, 16 (1941).

[21] E. H. Lieb and F. Y. Wu, in *Phase Transition and Critical Phenomena*, edited by C. Domb and M. S. Green, (Academic, London, 1972), Vol. 1.

[22] R. J. Baxter, *Exactly Solvable Models in Statistical Physics* (Academic, London, 1982).

[23] Instead of ω_5 and ω_6 we could have taken ω_7 and ω_8, the corresponding two extra vertices of the eight-vertex model. But, the two models so constructed are identical, as they can be transformed into each other by a unitary transformation; see E. Barouch in *Phase Transitions and Critical Phenomena* (Ref. [21]).

[24] H. van Beijeren, Phys. Rev. Lett. **38**, 993 (1977).

[25] W. K. Burton and N. Cabrera, Disc. Faraday Soc. **5**, 40 (1949); W. K. Burton, N. Cabrerea, and F. C. Frank, Philos. Trans. R. Soc. London Ser. A **243**, 299 (1951).

[26] E. H. Hauge and P. C. Hemmer, Physica Norvegica **5**, 209 (1974); and C. Deutsch and M. Lavaud, Phys. Rev. A **9**, 2598 (1974).

[27] C. Jayaprakash and W. F. Saam, Phys. Rev. B **30**, 3917 (1984).

[28] A. Trayanov, A. C. Levi, and E. Tosatti, Surf. Sci. **233**, 184 (1990).

[29] C. Garrod, A. C. Levi, and M. Touzani, Solid State Commun. **75**, 375 (1990); C. Garrod, Phys. Rev. A **41**, 4184 (1990).

[30] N. A. Gjostein, in *Surfaces and Interfaces: Chemical and Physical Characteristics*, edited by J. J. Burke, N. L. Reed, and V. Weiss (Syracuse University Press, Syracuse, NY, 1967).

[31] L.-H. Gwa and H. Spohn (unpublished).

[32] M. Gaudin, *La Fonction d'Onde de Bethe* (Masson, Paris, 1983).

[33] These equations are identical to those given in Ref. [32], with the obvious change $\omega_3 \leftrightarrow \omega_4$, due to the different notation used. For a further generalization, see R. J. Baxter, Stud. Appl. Math. **50**, 51 (1971).

[34] Even if we had chosen them not to be equal, we could transform the transfer matrix by a similarity transformation, see E. Barouch in Ref. [21], to make them equal.

[35] We have chosen $\omega_2 = 0$, in order that our result can be easily mapped to surface and growth models. Obviously, any of the first four Boltzmann weights can be chosen to

be zero. The solution can be easily transformed from one case to another.

[36] F. Y. Wu, Phys. Rev. Lett. **18**, 605 (1967); Phys. Rev. **168**, 539 (1967).

[37] C. P. Yang, Phys. Rev. Lett. **19**, 586 (1967); B. Sutherland, C. N. Yang, and C. P. Yang, *ibid.* **19**, 588 (1967).

[38] C. N. Yang and C. P. Yang, Phys. Rev. **150**, 321 (1966); **150**, 327 (1966).

[39] A. P. Prudnikov, Yu. A. Brychkov, and O. I. Marichev, *Integrals and Series* (Gordon and Breach, New York, 1986), Vol. 1. The $f(\theta)$ notation can also be found in *Handbook of Mathematical Functions*, edited by M. Abramowitz and I. A. Stegun (Dover, New York, 1970).

[40] I. S. Gradshteyn and I. M. Ryzhik, *Table of Integrals, Series, and Products* (Academic, San Diego, 1980).

[41] F. Y. Wu, Phys. Rev. B **3**, 3895 (1971); see also Ref. [21], p. 439.

[42] See Eqs. (356) and (307b) of Ref. [21], or Eqs. (4.3.9) and (4.3.21) of I. Nolden, Ph.D. thesis, University of Utrecht, 1990. Many of the derivations and results presented in the above-mentioned thesis there have never been published in the literature before.

[43] $F(y) = [y/(1+y)] \ln |1 - (1-y^2)/[y(1-2y)]|$.